

This is a self-archived version of an original article. This version may differ from the original in pagination and typographic details.

Author(s): Maas, Huub; Noort, Wendy; Baan, Guus C.; Finni, Taija

Title: Non-uniformity of displacement and strain within the Achilles tendon is affected by joint angle configuration and differential muscle loading

Year: 2020

Version: Accepted version (Final draft)

Copyright:

Rights: CC BY-NC-ND 4.0

Rights url: <https://creativecommons.org/licenses/by-nc-nd/4.0/>

Please cite the original version:

Maas, H., Noort, W., Baan, G. C., & Finni, T. (2020). Non-uniformity of displacement and strain within the Achilles tendon is affected by joint angle configuration and differential muscle loading. *Journal of Biomechanics*, 101, Article 109634.
<https://doi.org/10.1016/j.jbiomech.2020.109634>

1 **Author Accepted Manuscript for publication:**

2 **Maas, Huub; Noort, Wendy; Baan, Guus C.; Finni, Taija (2020). Non-uniformity of**
3 **displacement and strain within the Achilles tendon is affected by joint angle**
4 **configuration and differential muscle loading. Journal of Biomechanics, In Press.**

5 **DOI: 10.1016/j.jbiomech.2020.109634**

6 -----

7 **Non-uniformity of displacement and strain within the Achilles tendon is affected by**
8 **joint angle configuration and differential muscle loading**

9 Huub Maas¹, Wendy Noort¹, Guus C. Baan¹, and Taija Finni²

10 ¹Department of Human Movement Sciences, Faculty of Behavioural and Movement
11 Sciences, Vrije Universiteit Amsterdam, Amsterdam Movement Sciences, The Netherlands

12 ²Neuromuscular Research Center, Faculty of Sport and Health Sciences, University of
13 Jyväskylä, Finland

14

15 3643 words

16

17 Corresponding author

18 Huub Maas, Department of Human Movement Sciences, Faculty of Behavioural and
19 Movement Sciences, Amsterdam Movement Sciences, Vrije Universiteit Amsterdam, The
20 Netherlands.

21 email: h.maas@vu.nl

22 **Abstract**

23 Although the Achilles tendon (AT) has been studied for more than a century, a complete
24 understanding of the mechanical and functional consequences of AT structural organization is
25 currently lacking. The aim of this study was to assess how joint angle configuration affects
26 subtendon displacement and strain of soleus (SOL) and lateral gastrocnemius (LG) muscles.
27 Knots sutured onto SOL and LG subtendons of 12 Wistar rats, were videotaped to quantify
28 displacements and the ankle torque was assessed for different isometric activation conditions
29 (i.e., individual and simultaneous) of the triceps surae muscles. Changing ankle and knee joint
30 angle affected the magnitude of displacement, relative displacement and strain of both SOL
31 and LG subtendons. SOL subtendon behavior was not only affected by changes in ankle angle,
32 but also by changes in knee angle. Displacement of SOL subtendon decreased (28-49%), but
33 strain increased in response to knee extension. Independent of joint angle configuration,
34 stimulation of any combination of the muscles typically resulted in displacements and strains
35 of LG and SOL subtendons. Typically SOL displaced more but LG displaced more when
36 stimulated at longer muscle lengths. Our results demonstrate that the distinct subtendons of the
37 Achilles tendon can move and deform differently, but are not fully independent. Within the
38 AT, there appears to be a precarious balance between sliding allowance and mechanical
39 connectivity between subtendons.

40

41 **Keywords:** shear, strain, displacement, ankle torque, Achilles tendon, soleus, gastrocnemius

42 **Introduction**

43 Although the Achilles tendon (AT) has been studied for more than a century, the interest in the
44 structure and function of its subtendons arising from the triceps surae muscles is rather recent.
45 These subtendons are distinct to a large degree and they rotate along the proximal-distal axis
46 (Cummins et al., 1946; Edama et al., 2015; Finni et al., 2018; Parsons, 1894; Szaro et al., 2009).
47 However, a complete understanding of the mechanical and functional consequences of this
48 structural organization is currently lacking. The presence of distinct subtendons of soleus
49 (SOL), lateral (LG) and medial gastrocnemius muscles (MG) may facilitate independent
50 transmission of muscle forces to the calcaneal bone and, hence, distinct mechanical effects of
51 each muscle at the ankle joint (Haraldsson et al., 2008).

52 Non-uniform displacements within the AT, as assessed using ultrasound-based methods,
53 have been reported during passive ankle movement (Arndt et al., 2012), during eccentric
54 loading of the calf muscles (Slane and Thelen, 2014) and during human walking (Franz et al.,
55 2015). In the distal part of the AT, the anterior (deep) portion is generally associated with the
56 SOL subtendon and the posterior (superficial) portion with the MG subtendon (Edama et al.,
57 2015; Szaro et al., 2009). The above results suggest some degree of independence between AT
58 subtendons, but in human studies unequivocal identification of the individual AT subtendons
59 is not yet possible.

60 While non-uniform displacements within the AT indicate some degree of independence
61 between AT subtendons, it does not exclude some connectivity. Relative sliding of the
62 subtendons will strain the inter-subtendon matrix, which may result in force transmission
63 between the subtendons. The matrix between fascicles within equine (Thorpe et al., 2015) and
64 rat Achilles tendons (Maas et al., 2018) was found to be of sufficient strength to bear forces
65 when substantial sliding (i.e. 5-8% of tendon length) occurs. Recently, it was shown that by
66 activating SOL muscle selectively, or all triceps surae muscles together, SOL subtendon

67 strained more than LG subtendon. On the other hand, when LG muscle was selectively
68 stimulated, LG subtendon strained more than SOL subtendon although they underwent similar
69 overall displacement. (Finni et al., 2018). This suggests indirectly, that while force transmission
70 via the inter-subtendon matrix is possible, there is also flexibility in the system allowing
71 movement within the tendon.

72 Several factors could contribute to the non-uniform deformations of AT subtendons. The
73 stiffness of the subtendons could be different, for which there is some indirect evidence (Farris
74 et al., 2013; Finni et al., 2018; Lichtwark et al., 2013; Obst et al., 2016). The subtendons could
75 be loaded by different muscle forces (Arndt et al., 1999; Arndt et al., 1998; Handsfield et al.,
76 2017), which could be caused by differential muscle activation or the muscles acting at
77 different parts of their length-force curves. Because SOL does not span the knee joint, the
78 length and relative position of gastrocnemius muscle can be modified independently by
79 changes of knee joint angle. In our previous study, we investigated effects of differential
80 muscle activation on subtendon deformations, but kept the position of the knee and ankle joints
81 constant (Finni et al., 2018). In humans, several previous studies involving both passive and
82 active muscle conditions reported no effects of knee joint angle on non-uniformities in the
83 displacement within the AT (Bogaerts et al., 2018; Franz and Thelen, 2015; Stenroth et al.,
84 2019). Effects of knee angle on strains within the various subtendons of the AT have not been
85 studied.

86 Therefore, the aim of this study was to assess how joint angle configuration (affecting
87 muscle length and relative position) affects SOL and LG subtendon behavior (i.e.,
88 displacement, relative displacement and strain). This aim was tested for different activation
89 conditions (i.e., individual and simultaneous) of the triceps surae muscles. We hypothesized
90 that changes in knee angle will not only affect deformations of LG subtendon, but also of SOL
91 subtendon behavior.

92

93

94

95 **Methods**

96 *Animals*

97 Data were obtained from 12 adult male Wistar rats (235.5 ± 16.5 g). Surgical and experimental
98 procedures followed the guidelines and regulations concerning animal welfare and
99 experimentation set forth by the Dutch law and were approved by the institutional Committee
100 on Ethics of Animal Experimentation at the Vrije Universiteit Amsterdam (#FBW12-01).

101 According to standard procedures in our laboratory (Maas et al., 2001), the rats were
102 deeply anesthetized by intraperitoneal injection of urethane solution (1.2 ml/100g body mass,
103 12.5% urethane solution). If withdrawal reflexes could still be elicited, supplemental doses
104 (0.3–0.5 ml/time) were administered. Animals were placed on an electrical heating pad to keep
105 their core temperature at approximately 37°C. After completion of the experiments, the animals
106 were euthanized with an overdose of pentobarbital sodium (Euthasol 20%) injected
107 intracardially, and double-sided pneumothorax.

108

109 *Surgical preparations and fixation in experimental setup*

110 Surgical procedures were the same as those described previously (Finni et al., 2018). This study
111 also revealed that the morphology of rat AT is very similar to that of human AT. The left
112 hindlimb was shaved. The skin covering the lower leg and the biceps femoris were removed.
113 The femur was exposed for later fixation of a clamp. Anatomical landmarks for axis of rotation
114 of ankle (medial and lateral malleoli) and knee joints (origin of medial and lateral collateral
115 ligament) were identified and marked with a permanent marker (Tijs et al., 2014). The AT was
116 freed from all connective and fat tissues leaving the insertion to the calcaneal bone intact. For

117 assessment of tendon deformations, four knotted suture markers (Mariderm Schwarz, 7/0,
118 Catgut GmbH, Germany) were sutured into each of the LG and SOL subtendons (Fig. 1). All
119 exposed tissues were regularly irrigated with saline.

120 The foot was attached to a 6 degrees-of-freedom load cell (Mini40-E, ATI, Apex, NC,
121 USA) and the femur was rigidly secured to the setup (for details see Tijs et al., 2014). The
122 center of rotation of ankle and knee joint were aligned with the set-up's rotational axes. The
123 set-up allowed for manipulation of ankle and knee joint angles in the sagittal plane exclusively
124 (Fig. 1). Wire electrodes for intramuscular stimulation were placed near the neuromuscular
125 junctions of SOL, LG and medial gastrocnemius (MG) muscles (for details see Tijs et al., 2014,
126 2016). As the threshold current near a motor endplate is substantially lower than direct
127 excitation of muscle fibers (Mortimer and Bhadra, 2004), the chance of excitation of
128 surrounding muscles was minimized. A video camera (HC-V720, Panasonic, UK) was placed
129 orthogonal to the sagittal plane with focus on the AT. A ruler was placed below the tendon
130 from which 5 mm length was digitized and used for calibration, which yielded an average
131 resolution of 0.023 mm/pixel (range 0.022-0.024).

132

133 *Experimental protocol*

134 For each muscle, stimulation intensity was defined as the intensity resulting in the highest
135 twitch torque. Two conditioning twitches with 1s in between were followed by a 1s tetanic
136 stimulus (stimulation frequency 100Hz, pulse width 100 μ s). Two minutes rest was given
137 between contractions. To monitor changes in muscle force producing capacity, control trials
138 with ankle and knee joints at 90° (A90K90) with all SOL+LG+MG muscles stimulated were
139 performed before, three times during and after the experiment. There was no effect of time on
140 control torques ($p=0.970$, repeated measures ANOVA), and the post control trial (39.5 ± 6.7
141 mNm) was not significantly different from the pre control (39.9 ± 8.5 mNm; $p=0.807$, paired t-

142 test). During each contraction, forces and moments measured by the load cell (sampled at
143 1000Hz) and images of the AT (50 frames/s) were acquired.

144 Marker displacements and ankle joint moments were assessed for four different joint
145 configurations and four muscle stimulation conditions of which the order was randomized
146 between animals. The four joint angle configurations were: (i) ankle joint at 120° and knee
147 joint at 60° (A120K60), (ii) ankle joint at 120° and knee joint at 90° (A120K90), (iii) ankle
148 joint at 120° and knee joint at 120° (A120K120), (iv) ankle joint at 90° and knee joint at
149 90° (A90K90). Note that in the (i), (ii) and (ii) conditions only the knee angle is manipulated,
150 changing the length of LG and MG but not that of SOL (Fig. 1). The four muscle stimulation
151 conditions were: (i) SOL only, (ii) SOL, LG and MG together, (iii) LG and MG together, (iv)
152 LG only.

153

154

155 **Data analysis**

156 Three-dimensional gravity-corrected ankle torques were calculated following previously
157 described procedures (Tijs et al., 2014). Passive torque was obtained from a 50ms time window
158 in relaxed condition (after the second twitch). This was subtracted from the torque obtained
159 from a 50ms window during the tetanic contraction to obtain the active torque used in the
160 statistical analysis.

161 An image captured in the relaxed condition (after the second twitch corresponding to the
162 passive torque) and an image during the tetanic contraction (corresponding to the time of active
163 torque) were extracted for further analysis of tendon marker displacements. From these two
164 images, the tendon markers were digitized manually by selecting the centroid of the knot (Finni

165 et al., 2018), and [x,y] coordinates were extracted. Image analysis was done using custom
166 written software in MATLAB (R2014b, Mathworks, Natick, MA, USA).

167 From the [x,y] coordinates, displacement (D) of each of the markers (n) from passive to
168 active state (Δx and Δy) was calculated. Then the average displacement (\bar{D}) was calculated as
169 the mean of the four SOL and four LG marker displacements, respectively.

$$170 \quad D_n = \sqrt{\Delta x_n^2 + \Delta y_n^2} \quad n = 1,2,3,4$$

$$171 \quad D = \frac{D_1 + D_2 + D_3 + D_4}{4}$$

172 Relative displacement (ΔD) was calculated as:

$$173 \quad D = D_{LG} - D_{SOL}$$

174 Strains (ϵ) based on a linear 3-segment model connecting the four markers in SOL and
175 LG subtendons, respectively, were calculated as $\epsilon = (L-L_0)/L_0$, where L was the 3-segment
176 length in an active state and L_0 the 3-segment length in the passive state.

177 Average LG and SOL muscle-tendon unit lengths were estimated (Fig. 1) using an ankle-
178 knee geometric model (Bernabei et al., 2017). The following anatomical parameters, required
179 in the model, were measured from the animals of the present study: ankle lever arm length
180 (6.8mm, SD 0.69) and tibia length (38.3mm, SD 1.01).

181

182 *Statistics*

183 Normal distribution of the data was checked with the Shapiro-Wilk test, by comparing mean
184 and median values, and by checking values of skewness and kurtosis. There was no strong
185 evidence for non-normal distribution and parametric statistics were used. A two-way repeated
186 measures ANOVA (joint configuration \times stimulation) was used to examine differences in
187 torque and relative displacement between conditions (Huyhn-Feldt correction was used in case
188 of violation of sphericity). The effects of joint configuration on average displacement and

189 within subtendon strains of SOL and LG subtendons was examined separately at each
190 stimulation condition with two-way repeated measures ANOVAs (joint configuration \times
191 subtendon). In case of significant interaction, Bonferroni corrected t-tests were performed (i.e.
192 p-values were multiplied by the number of comparisons). Effect sizes from ANOVA (Partial
193 Eta Squared, η^2_{partial}) are reported. Level of significance was set at $p \leq 0.05$.

194

195 **Results**

196 *Ankle joint torque*

197 There were main effects of joint configuration ($p=0.034$, $\eta^2_{\text{partial}}=0.279$) and stimulation
198 ($p<0.001$, $\eta^2_{\text{partial}}=0.965$) on ankle torque, and a significant interaction ($p=0.001$, $\eta^2_{\text{partial}}=0.359$)
199 (Fig. 2). Pairwise comparisons revealed overall effects of joint configuration on torque only
200 between A120K90 and A90K90 ($p=0.004$), torques being higher in the latter condition. All
201 stimulation conditions produced significantly different torques at each angle (all $p<0.001$).

202 *Subtendon displacement*

203 When SOL was stimulated, displacements of SOL and LG subtendons were different ($p=0.001$,
204 $\eta^2_{\text{partial}}=0.650$). There was also a main effect of joint configuration ($p<0.001$, $\eta^2_{\text{partial}}=0.663$),
205 but no significant interaction ($p=0.083$, $\eta^2_{\text{partial}}=0.198$) (Fig. 3A). Pairwise comparisons
206 revealed that SOL displacement was greater than LG displacement (ranging from 23% to 93%)
207 at each joint configuration tested ($p \leq 0.010$).

208 When SOL+LG+MG were stimulated, displacements of SOL and LG subtendons were
209 different ($p=0.003$, $\eta^2_{\text{partial}}=0.571$), there was a main effect of joint configuration ($p<0.001$,
210 $\eta^2_{\text{partial}}=0.658$) and a significant interaction ($p=0.002$, $\eta^2_{\text{partial}}=0.364$) (Fig. 3B). Pairwise
211 comparisons revealed that SOL displacement was greater than LG at joint configurations
212 A120K60 (7%, $p=0.004$), A120K90 (6%, $p=0.002$) and A120K120 (6%, $p=0.013$).

213 When LG+MG were stimulated, displacements of SOL and LG subtendons were different
214 ($p=0.030$, $\eta^2_{\text{partial}}=0.362$), there was a main effect of joint configuration ($p<0.001$,
215 $\eta^2_{\text{partial}}=0.712$), and a significant interaction ($p<0.001$, $\eta^2_{\text{partial}}=0.537$) (Fig. 3C). Pairwise
216 comparisons indicated that LG displacement was greater than SOL at A120K120 (7%,
217 $p=0.009$) and A90K90 (20%, $p=0.001$).

218 When LG was stimulated, SOL and LG subtendon displacements were similar ($p=0.747$,
219 $\eta^2_{\text{partial}}=0.010$), but there was a main effect of joint configuration ($p<0.001$, $\eta^2_{\text{partial}}=0.662$), and
220 a significant interaction ($p<0.001$, $\eta^2_{\text{partial}}=0.499$) (Fig. 3D). Pairwise comparisons indicated
221 that SOL displaced 6% more than LG at A120K60 ($p=0.044$), but at A90K90 LG displacement
222 was 21% greater than SOL ($p=0.022$).

223 These results indicate that joint angle configuration affects subtendon displacement both
224 when muscles are stimulated and when some of the muscles were passive. Displacement of
225 SOL subtendon was significantly affected by changes in knee angle (all $p\leq 0.011$).

226

227 *Relative displacement between subtendons*

228 Main effects of joint configuration ($p<0.001$, $\eta^2_{\text{partial}}=0.503$) and stimulation ($p=0.002$,
229 $\eta^2_{\text{partial}}=0.552$) on relative subtendon displacement were found, without significant interaction
230 ($p=0.068$, $\eta^2_{\text{partial}}=0.162$). Pairwise comparisons revealed overall differences in relative
231 displacement at joint configurations of A120K60 vs. A90K90 ($p=0.009$) and A120K90 vs.
232 A90K90 ($p=0.012$), relative displacements being higher (i.e. LG moved more than SOL
233 subtendon) in the A90K90 condition (Fig. 4). These results indicate that relative displacement
234 between SOL and LG subtendons is affected independently by joint configuration as well as
235 stimulation condition.

236

237 *Subtendon strain*

238 When SOL was stimulated, strains of SOL and LG subtendons were different ($p < 0.001$,
239 $\eta^2_{\text{partial}} = 0.879$), there was a main effect of joint configuration ($p = 0.001$, $\eta^2_{\text{partial}} = 0.402$) and a
240 significant interaction ($p < 0.001$, $\eta^2_{\text{partial}} = 0.583$). Pairwise comparisons indicated that at each
241 joint configuration SOL strain was several times (77-479%) greater than LG strain ($p \leq 0.025$).

242 When SOL+LG+MG was stimulated, strains of SOL and LG subtendons were different
243 ($p = 0.003$, $\eta^2_{\text{partial}} = 0.563$), there was a main effect of joint configuration ($p < 0.001$,
244 $\eta^2_{\text{partial}} = 0.473$) and a significant interaction ($p < 0.001$, $\eta^2_{\text{partial}} = 0.633$). Pairwise comparisons
245 revealed that strain in SOL subtendon was greater than in LG at A120K90 (79%, $p = 0.001$),
246 A120K120 (116%, $p < 0.001$) and A90K90 (68%, $p = 0.011$).

247 When LG+MG was stimulated, strains of SOL and LG subtendons were different ($p < 0.001$,
248 $\eta^2_{\text{partial}} = 0.856$), there was a main effect of joint configuration ($p = 0.031$, $\eta^2_{\text{partial}} = 0.234$) and a
249 significant interaction ($p < 0.001$, $\eta^2_{\text{partial}} = 0.677$). Pairwise comparisons showed that strain in
250 LG was several times greater than in SOL at each joint configuration ($p \leq 0.01$).

251 When LG was stimulated, strains of SOL and LG subtendons were different ($p < 0.001$,
252 $\eta^2_{\text{partial}} = 0.925$), there was a main effect of angle ($p = 0.014$, $\eta^2_{\text{partial}} = 0.271$) and a significant
253 interaction ($p < 0.001$, $\eta^2_{\text{partial}} = 0.666$). Pairwise comparisons indicated that the strain in LG was
254 several times greater than in SOL at each joint configuration ($p < 0.001$).

255 Maximum strains were observed at the shortest muscle-tendon unit lengths tested for LG.
256 For LG, maximum strain ($6.3 \pm 1.8\%$) was observed during LG stimulation at A120K60.
257 Maximum SOL strain ($8.5 \pm 2.2\%$) was found during SOL stimulation at A120K120 (Fig. 5).
258 As found for displacement, SOL subtendon strain was affected by changes in knee joint angle
259 (all stimulation conditions $p < 0.015$).

260

261

262 **Discussion**

263 The main finding of this study was consistent with the hypothesis showing that the joint
264 angle configuration affected the magnitude of displacement, relative displacement and strain
265 of both SOL and LG subtendons. More specifically, SOL subtendon behavior was not only
266 affected by changes in ankle angle, but also by changes in knee angle. Independent of joint
267 angle configuration, stimulation of any combination of the muscles typically resulted in
268 displacements and strains of both subtendons. Most often the SOL subtendon displaced more,
269 but LG subtendon displaced more when LG was stimulated at longer muscle lengths (Fig. 3).
270 Strain in the SOL or LG subtendon was greater when their representative muscle was
271 stimulated. When all muscles were stimulated, typically SOL subtendon strained more than
272 LG. As reported previously for the rat (Finni et al., 2018) and human AT (e.g. Arndt et al.,
273 2012; Beyer et al., 2018; Franz et al., 2015; Slane and Thelen, 2014), we found SOL and LG
274 subtendons to displace and strain differently in most conditions tested. Both SOL and LG
275 subtendon displacements decreased when knee was extended and reached smallest
276 displacement to each stimulation condition at the longest muscle-tendon unit lengths (Fig. 3),
277 which is in agreement with the stress-strain properties of tendon (Cui et al., 2009). We also
278 found that the relative displacement between SOL and LG subtendons was affected
279 independently by knee angle/joint configuration (Fig. 4). This is in contrast with several studies
280 in human subjects in which no significant effects of knee angle on non-uniform displacements
281 within the human AT were reported (Bogaerts et al., 2018; Franz and Thelen, 2015; Stenroth
282 et al., 2019). This may be explained by differences in the location along the AT for which local
283 deformations were assessed, being more proximal in our study compared to most studies in
284 humans. It has been suggested that the subtendons are more tightly linked distally than
285 proximally (Arndt et al., 1999).

286 A recent human study showed that SOL subtendon displaced more than LG at the different
287 ankle joint angles tested and this corresponded to greater shortening of SOL than LG muscle
288 (Clark and Franz, 2018). Indeed, it is to be expected that if a muscle is selectively stimulated,
289 its representative tendon would move more than others. In the present study, when LG was
290 stimulated at the longest length (A90K90), LG subtendon displacement was greater than SOL
291 (Fig. 4). However, when LG was stimulated at the shortest length (A120K60), SOL displaced
292 more than LG. This suggests that the sign of relative subtendon displacement is not only
293 dependent on the level of muscle contraction. This is in contrast to strain, which was always
294 greater when their representative muscle was stimulated; maximal strain being higher in SOL
295 (up to ~8%) than in LG subtendon (up to ~6%). Humans studies have reported strains ranging
296 from 3.8-6.6% in SOL to 2.6-2.7% in MG (see Finni et al., 2018). However, the strain responses
297 to changes in joint configuration differed between subtendons. Greatest strains in SOL were
298 found at A120K90 and A120K120, while greatest LG strains were found at A120K60 (Fig 5).

299 Consistent with our hypothesis, changes in knee angle did not only affect deformations of
300 LG subtendon, but also of SOL subtendon. The differential behaviour between subtendons
301 when joint configuration was altered, likely relates to force transmission within and between
302 the involved tissues which can be modified by a number of factors.

303 Firstly, force can be transmitted between gastrocnemius and SOL muscle bellies (Bernabei
304 et al., 2015) and/or subtendons (Maas et al., 2018). Knee movements will change the position
305 of gastrocnemius relative to SOL and, thereby, strain connective tissues between the muscle
306 bellies (Bojsen-Moller et al., 2010; Maas, 2009; Maas and Finni, 2018). A recent human study
307 showed that selective activation of LG muscle can stiffen the connective tissues between SOL
308 and LG muscle bellies, thereby, facilitating force transmission at least at short muscle lengths
309 (Finni et al. 2017). Thus, both the relative muscle positions and activation may change the

310 extent of intermuscular force transmission and, hence, force levels exerted at each of the
311 subtendons.

312 Secondly, knee movements will affect the length of gastrocnemius subtendon and, thereby,
313 the relative position with SOL subtendon. This will cause shear within the inter-subtendon
314 matrix, which may facilitate inter-subtendon force transmission. Such force transmission is
315 supported also by other observations; both subtendons moved when only one muscle was
316 stimulated. Thus, force exerted by the stimulated muscle did not only pull on the corresponding
317 subtendon but also on the other one.

318 Displacements do not provide information about the magnitude of the forces involved, but
319 SOL stimulation resulted also in substantial strains in LG subtendon. In addition, SOL
320 subtendon strain was found in response to LG stimulation, but to a smaller degree. As strain is
321 a function of stress, these results indicate that part of the force produced by the muscle fibers
322 in one muscle is transmitted via the inter-subtendon matrix to the subtendon of the neighboring
323 muscle.

324 Differences in strain between SOL and LG subtendons were substantially higher than
325 differences in displacement. When both LG and MG were stimulated simultaneously, strain
326 was observed in LG subtendon exclusively in three of the joint configurations, indicating that
327 the proximal portion of SOL subtendon was not deformed. Although it is clear that the SOL
328 and LG subtendons exert some force on each other resulting in similar displacements, the
329 strains suggest that most force produced by each muscle is transmitted via its own subtendon.

330 It should be noted that displacements and strains were assessed for only part of the AT, the
331 most proximal portion of SOL subtendon and the mid-portion of LG subtendon. The
332 mechanical effects of relative displacements proximally may be more pronounced distally. In
333 addition, marker displacements were measured in two-dimensions. Out-of-plane movements,
334 for example due to possible rotation of the tendon, were not captured (see also Finni et al.,

335 2018). This may explain the observed negative strains in SOL subtendon in response to
336 stimulation of LG and LG+MG muscles (Fig. 5).

337 Sliding within AT may be necessary to allow muscles crossing one (SOL) or two joints
338 (gastrocnemius) with independent activation patterns (Moritani et al., 1991) to function
339 normally, and lack of sliding may be a sign of malfunction. In a surgically repaired tendon,
340 relative displacements were reported to be completely absent even one year post-surgery
341 (Beyer et al., 2018) which may be due to scar tissue. On the other hand, because the inter-
342 subtendon matrix can bear considerable loads (Maas et al., 2018) forces produced by the triceps
343 surae can be distributed within the whole AT. We proposed recently that the inter-subtendon
344 matrix provides an alternative pathway for force transmission and may serve to minimize peak
345 stresses and, thereby, may prevent tendon injuries (Maas and Finni, 2018). The above suggests
346 a precarious balance between sliding allowance and mechanical connectivity between fascicles
347 and subtendons within the AT.

348 As a conclusion, our results demonstrate that the distinct subtendons of the Achilles tendon
349 can move and deform differently, but are not fully independent. SOL subtendon displacement
350 and strain were affected by knee joint angle that was likely due to force transmission via the
351 intermuscular and intersubtendon matrices. Subtendon strain was affected by changes in joint
352 configuration and muscle stimulation differently than subtendon displacement.

353

354 **Acknowledgements**

355 We thank Michel Bernabei for his help with the video analysis and Chris Tijs for his help with
356 the joint torque analysis.

357

358 **References**

359 Arndt, A., Bengtsson, A.S., Peolsson, M., Thorstensson, A., Movin, T., 2012. Non-uniform
360 displacement within the Achilles tendon during passive ankle joint motion. *Knee Surg. Sports*
361 *Traumatol. Arthrosc.* 20, 1868-1874.

362 Arndt, A., Bruggemann, G.P., Koebke, J., Segesser, B., 1999. Asymmetrical loading of the human
363 triceps surae: I. Mediolateral force differences in the Achilles tendon. *Foot Ankle Int.* 20, 444-449.

364 Arndt, A.N., Komi, P.V., Bruggemann, G.P., Lukkariniemi, J., 1998. Individual muscle contributions to
365 the in vivo achilles tendon force. *Clin Biomech (Bristol, Avon)* 13, 532-541.

366 Bernabei, M., Dieën, J.H.v., Maas, H., 2017. Longitudinal and transversal displacements between
367 triceps surae muscles during locomotion of the rat. *J. Exp. Biol.* 220, 537-550.

368 Bernabei, M., van Dieen, J.H., Baan, G.C., Maas, H., 2015. Significant mechanical interactions at
369 physiological lengths and relative positions of rat plantar flexors. *J. Appl. Physiol.* 118, 427-436.

370 Beyer, R., Agergaard, A.S., Magnusson, S.P., Svensson, R., 2018. Speckle tracking in healthy and
371 surgically repaired human Achilles tendons at different knee angles—A validation using implanted
372 tantalum beads. *Translational Sports Medicine* 1, 79-88.

373 Bogaerts, S., De Brito Carvalho, C., De Groef, A., Suetens, P., Peers, K., 2018. Non-uniformity in pre-
374 insertional Achilles tendon is not influenced by changing knee angle during isometric contractions.
375 *Scand. J. Med. Sci. Sports* 28, 2322-2329.

376 Bojsen-Moller, J., Schwartz, S., Kalliokoski, K.K., Finni, T., Magnusson, S.P., 2010. Intermuscular force
377 transmission between human plantarflexor muscles in vivo. *J. Appl. Physiol.* 109, 1608-1618.

378 Clark, W.H., Franz, J.R., 2018. Do triceps surae muscle dynamics govern non-uniform Achilles tendon
379 deformations? *PeerJ* 6, e5182.

380 Cui, L., Maas, H., Perreault, E.J., Sandercock, T.G., 2009. In situ estimation of tendon material
381 properties: differences between muscles of the feline hindlimb. *J. Biomech.* 42, 679-685.

382 Cummins, E.J., Anson, B.J., Carr, B.W., Wright, R.R., Hauser, E.D.W., 1946. The Structure of the
383 Calcaneal Tendon (of Achilles) in Relation to Orthopedic Surgery - with Additional Observations on
384 the Plantaris Muscle. *Surgery Gynecology & Obstetrics* 83, 107-116.

385 Edama, M., Kubo, M., Onishi, H., Takabayashi, T., Inai, T., Yokoyama, E., Hiroshi, W., Satoshi, N.,
386 Kageyama, I., 2015. The twisted structure of the human Achilles tendon. *Scand. J. Med. Sci. Sports*
387 25, e497-503.

388 Farris, D.J., Trewartha, G., McGuigan, M.P., Lichtwark, G.A., 2013. Differential strain patterns of the
389 human Achilles tendon determined in vivo with freehand three-dimensional ultrasound imaging. *J.*
390 *Exp. Biol.* 216, 594-600.

391 Finni, T., Bernabei, M., Baan, G.C., Noort, W., Tijs, C., Maas, H., 2018. Non-uniform displacement and
392 strain between the soleus and gastrocnemius subtendons of rat Achilles tendon. *Scand. J. Med. Sci.*
393 *Sports* 28, 1009-1017.

394 Franz, J.R., Slane, L.C., Rasske, K., Thelen, D.G., 2015. Non-uniform in vivo deformations of the
395 human Achilles tendon during walking. *Gait Posture* 41, 192-197.

396 Franz, J.R., Thelen, D.G., 2015. Depth-dependent variations in Achilles tendon deformations with age
397 are associated with reduced plantarflexor performance during walking. *J Appl Physiol (1985)* 119,
398 242-249.

399 Handsfield, G.G., Inouye, J.M., Slane, L.C., Thelen, D.G., Miller, G.W., Blemker, S.S., 2017. A 3D model
400 of the Achilles tendon to determine the mechanisms underlying nonuniform tendon displacements.
401 *J. Biomech.* 51, 17-25.

402 Haraldsson, B.T., Aagaard, P., Qvortrup, K., Bojsen-Moller, J., Krogsgaard, M., Koskinen, S., Kjaer, M.,
403 Magnusson, S.P., 2008. Lateral force transmission between human tendon fascicles. *Matrix Biol.* 27,
404 86-95.

405 Lichtwark, G.A., Cresswell, A.G., Newsham-West, R.J., 2013. Effects of running on human Achilles
406 tendon length-tension properties in the free and gastrocnemius components. *J. Exp. Biol.* 216, 4388-
407 4394.

408 Maas, H., 2009. Mechanical interactions between skeletal muscles, in: Shinohara, M. (Ed.), *Advances*
409 *in Neuromuscular Physiology of Motor Skills and Muscle Fatigue*. Research Signpost, Kerala, India,
410 pp. 285-302.

411 Maas, H., Baan, G.C., Huijing, P.A., 2001. Intermuscular interaction via myofascial force transmission:
412 effects of tibialis anterior and extensor hallucis longus length on force transmission from rat
413 extensor digitorum longus muscle. *J. Biomech.* 34, 927-940.

414 Maas, H., Cesa Correira, J., Baan, G.C., Noort, W., Screen, H.R., Year Force transmission between
415 achilles subtendons of rat In *World Congress of Biomechanics*. Dublin, Ireland.

416 Maas, H., Finni, T., 2018. Mechanical Coupling Between Muscle-Tendon Units Reduces Peak Stresses.
417 *Exerc. Sport Sci. Rev.* 46, 26-33.

418 Moritani, T., Oddsson, L., Thorstensson, A., 1991. Phase-dependent preferential activation of the
419 soleus and gastrocnemius muscles during hopping in humans. *J. Electromyogr. Kinesiol.* 1, 34-40.

420 Mortimer, J.T., Bhadra, N., 2004. Peripheral nerve and muscle stimulation, in: Horch, K.W., Dhillon,
421 G.S. (Eds.), *Neuroprosthetics: Theory and Practice*, Vol. 2 ed. World Scientific Publishing Company,
422 River Edge, NJ, pp. 638-682.

423 Obst, S.J., Newsham-West, R., Barrett, R.S., 2016. Changes in Achilles tendon mechanical properties
424 following eccentric heel drop exercise are specific to the free tendon. *Scand. J. Med. Sci. Sports* 26,
425 421-431.

426 Parsons, F.G., 1894. On the Morphology of the Tendo-Achillis. *J Anat Physiol* 28, 414-418.

427 Slane, L.C., Thelen, D.G., 2014. Non-uniform displacements within the Achilles tendon observed
428 during passive and eccentric loading. *J. Biomech.* 47, 2831-2835.

429 Stenroth, L., Thelen, D., Franz, J., 2019. Biplanar ultrasound investigation of in vivo Achilles tendon
430 displacement non-uniformity. *Transl Sports Med* 2, 73-81.

431 Szaro, P., Witkowski, G., Smigielski, R., Krajewski, P., Cizek, B., 2009. Fascicles of the adult human
432 Achilles tendon - an anatomical study. *Ann Anat* 191, 586-593.

433 Thorpe, C.T., Godinho, M.S., Riley, G.P., Birch, H.L., Clegg, P.D., Screen, H.R., 2015. The interfascicular
434 matrix enables fascicle sliding and recovery in tendon, and behaves more elastically in energy storing
435 tendons. *J Mech Behav Biomed Mater* 52, 85-94.

436 Tijs, C., van Dieen, J.H., Baan, G.C., Maas, H., 2014. Three-dimensional ankle moments and nonlinear
437 summation of rat triceps surae muscles. *PloS one* 9, e111595.

438 Tijs, C., van Dieen, J.H., Baan, G.C., Maas, H., 2016. Synergistic Co-activation Increases the Extent of
439 Mechanical Interaction between Rat Ankle Plantar-Flexors. *Front Physiol* 7, 414.

440

441 **Legends to Figures**

442

443 **Figure 1. Schematics of experimental setup and joint configurations.**

444 (A) Lateral view of the rat left hindlimb in the set-up. The femur was fixed and the foot was
445 attached to the load cell. Wire electrodes within soleus (SOL), medial (MG) and lateral
446 gastrocnemius (LG) muscle bellies were used for intramuscular stimulation. Knot sutures in
447 LG (top row) and SOL subtendons (bottom row) are shown as black dots. (B) Picture of
448 Achilles tendon in experimental setup showing the knot sutures in the lateral gastrocnemius

449 (top row of knots) and soleus subtendons (bottom row of knots). (C) A schematic of the rat
450 hind limb, indicating the different imposed angles of the ankle (A, 90° and 120°) and knee
451 joints (K, 60°, 90° and 120°). (D) Estimated muscle-tendon unit (MTU) lengths of LG and
452 SOL muscles for the four joint configurations (i.e., combinations of ankle and knee angles)
453 tested. As SOL muscle does not cross the knee joint, the MTU length of only LG will be altered
454 in three of the four joint configurations.

455

456 **Figure 2.** Effects of joint configuration (x-axis) and muscle stimulation condition (different
457 colour bars) on ankle plantarflexion torque. Each stimulation condition differed significantly
458 in each joint configuration. Overall differences in torque between joint angles (A, ankle; K,
459 knee) were found between A120K90 and A90K90 ($p=0.004$). SOL, soleus; LG, lateral
460 gastrocnemius; MG, medial gastrocnemius. ** indicates $p<0.01$. Means + SD are shown (n =
461 12).

462

463 **Figure 3.** Effects of joint configuration and muscle stimulation condition on displacement of
464 the subtendons of soleus (SOL) and lateral gastrocnemius (LG) muscles. Means + SD are
465 shown (n = 12). MG, medial gastrocnemius muscle. Significant differences between SOL and
466 LG subtendons: * $p<0.05$; ** $p<0.01$.

467

468 **Figure 4.** Relative displacement of soleus (SOL) and lateral gastrocnemius (LG) subtendons
469 for different joint configurations and stimulation conditions. Negative values mean that SOL
470 subtendon moved more than LG subtendon (see Methods). Means + SD are shown (n=12).
471 Significant differences between joint configurations: ** $p<0.01$. At a given joint angle
472 configuration, § indicates that the relative displacement for that stimulation condition was
473 significantly different ($p<0.05$) from that during SOL stimulation condition; # indicates a

474 difference with stimulation of ALL muscles and \$ indicates a difference with LG stimulation
475 condition.

476

477 **Figure 5.** Effects of joint configuration and muscle stimulation condition on strain of soleus
478 (SOL) and lateral gastrocnemius (LG) subtendons. Means + SD are shown (n = 12). Significant
479 differences between SOL and LG subtendon strain: * p<0.05, ** p<0.01,
480 *** p<0.001.

481

482 **Figure 6.** Effects of SOL muscle belly dissection on subtendon displacement and strain. X-
483 axis labels refer to LG or SOL tendon displacement (A) or strain (B) when SOL muscle belly
484 was intact or dissected. Data are reported for the various stimulation conditions. Means + SD
485 are shown (n = 8). *** p<0.001.

486

487 **Competing Interests**

488 None of the authors has any conflicts of interests.

489

490 **Funding**

491 This research was done during a visit from TF to HM, which was supported by a visitor's travel

492 grant from the Netherlands Organization for Scientific Research [040.11.519] and University

493 of Jyväskylä.

494

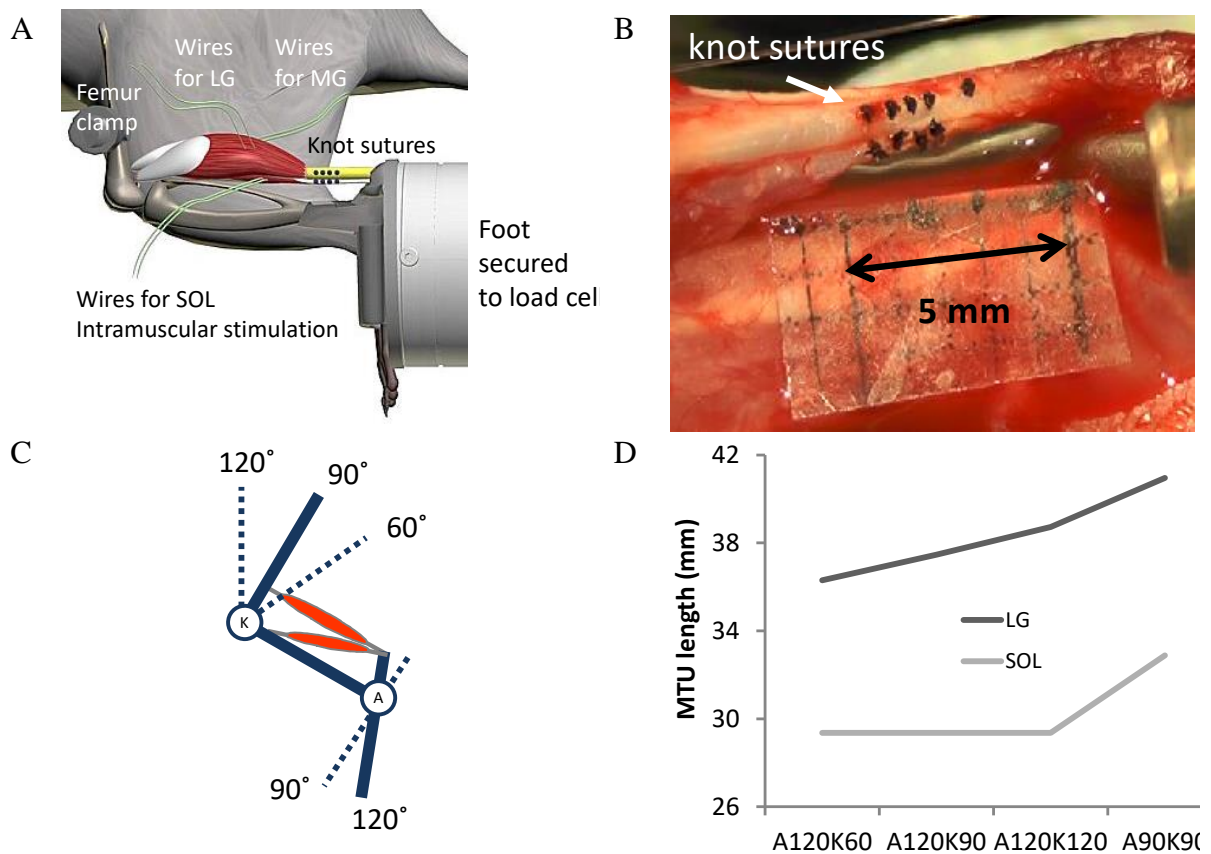


Figure 1. Schematics of experimental setup and joint configurations.

(A) Lateral view of the rat left hindlimb in the set-up. The femur was fixed and the foot was attached to the load cell. Wire electrodes within soleus (SOL), medial (MG) and lateral gastrocnemius (LG) muscle bellies were used for intramuscular stimulation. Knot sutures in LG (top row) and SOL subtendons (bottom row) are shown as black dots. (B) [Picture of Achilles tendon in experimental setup showing the knot sutures in the lateral gastrocnemius \(top row of knots\) and soleus subtendons \(bottom row of knots\).](#) (C) A schematic of the rat hind limb, indicating the different imposed angles of the ankle (A, 90° and 120°) and knee joints (K, 60°, 90° and 120°). (D) Estimated muscle-tendon unit (MTU) lengths of LG and SOL muscles for the four joint configurations (i.e., combinations of ankle and knee angles) tested. As SOL muscle does not cross the knee joint, the MTU length of only LG will be altered in three of the four joint configurations.

495

496

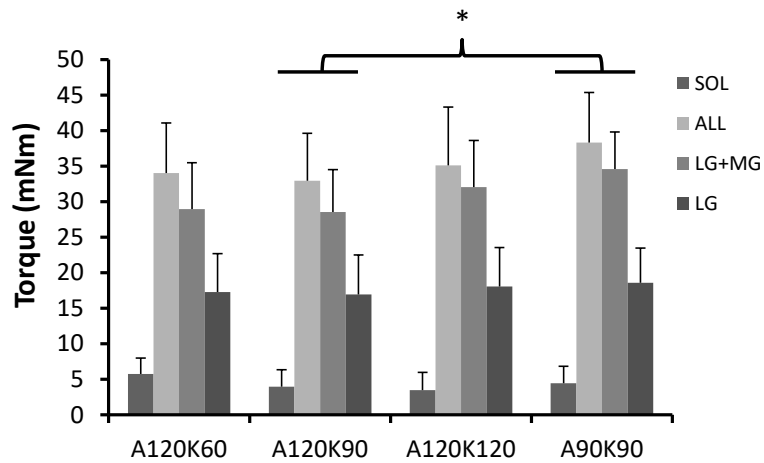


Figure 2. Effects of joint configuration (x-axis) and muscle stimulation condition (different colour bars) on ankle plantarflexion torque. Each stimulation condition differed significantly in each joint configuration. Overall differences in torque between joint angles (A, ankle; K, knee) were found between A120K90 and A90K90 ($p=0.004$). SOL, soleus; LG, lateral gastrocnemius; MG, medial gastrocnemius. ** indicates $p<0.01$. Means + SD are shown ($n = 12$).

497

498

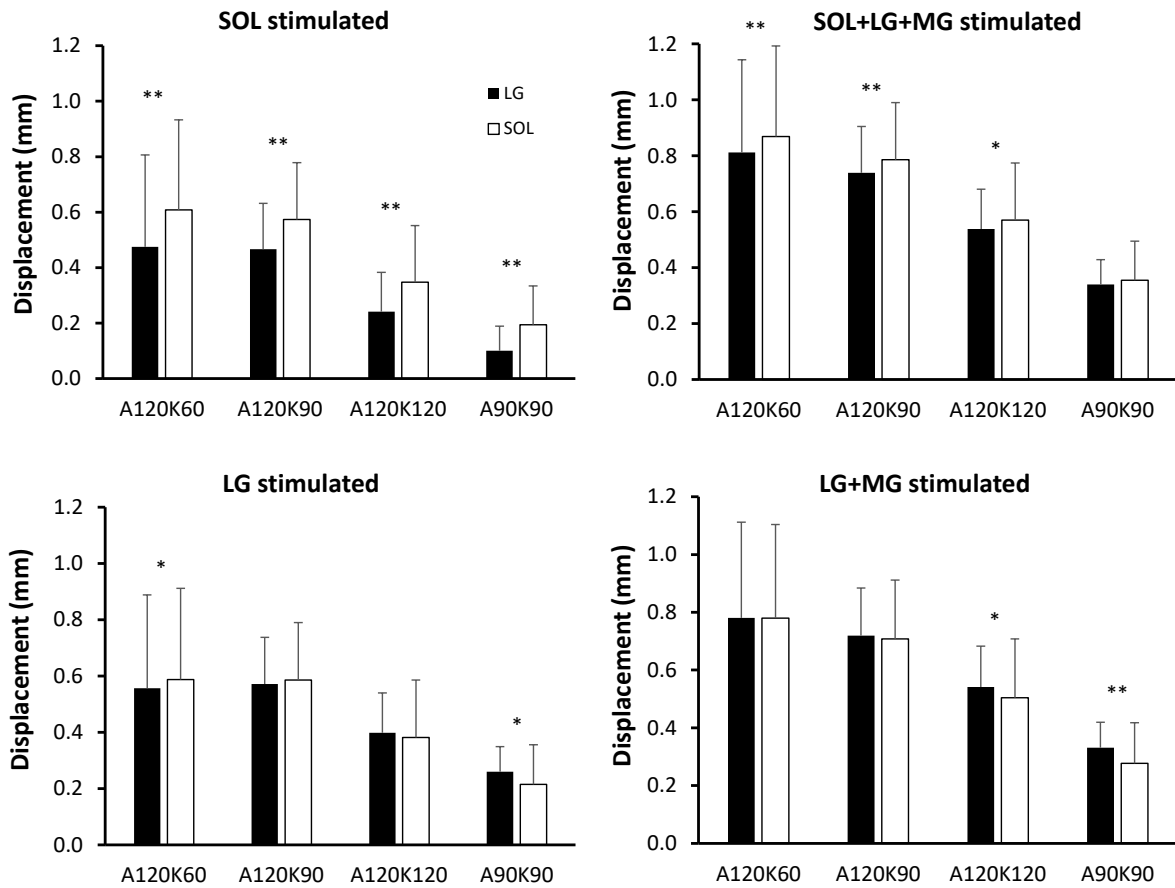


Figure 3. Effects of joint configuration and muscle stimulation condition on displacement of the subtendons of soleus (SOL) and lateral gastrocnemius (LG) muscles. Means + SD are shown (n = 12). MG, medial gastrocnemius muscle. Significant differences between SOL and LG subtendons: * p<0.05; ** p<0.01.

499

500

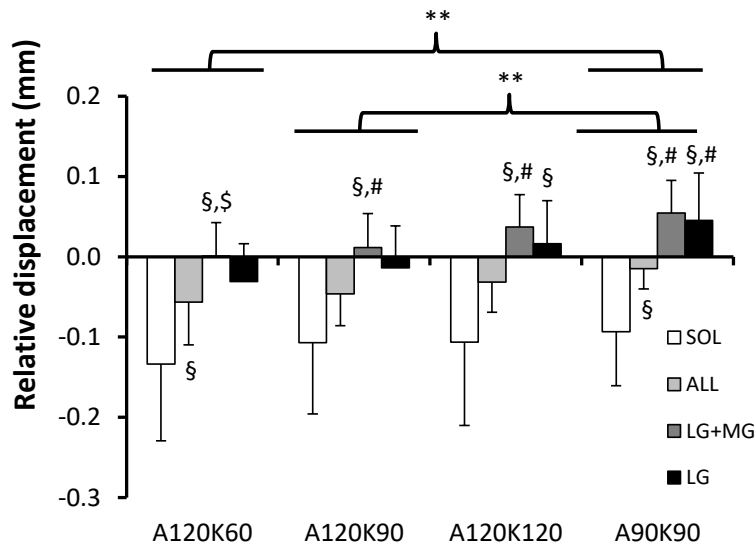


Figure 4. Relative displacement of soleus (SOL) and lateral gastrocnemius (LG) subtendons for different joint configurations and stimulation conditions. Negative values mean that SOL subtendon moved more than LG subtendon (see Methods). Means + SD are shown (n=12). Significant differences between joint configurations: ** p<0.01. At a given joint angle configuration, § indicates that the relative displacement for that stimulation condition was significantly different (p<0.05) from that during SOL stimulation condition; # indicates a difference with stimulation of ALL muscles and § indicates a difference with LG stimulation condition.

501

502

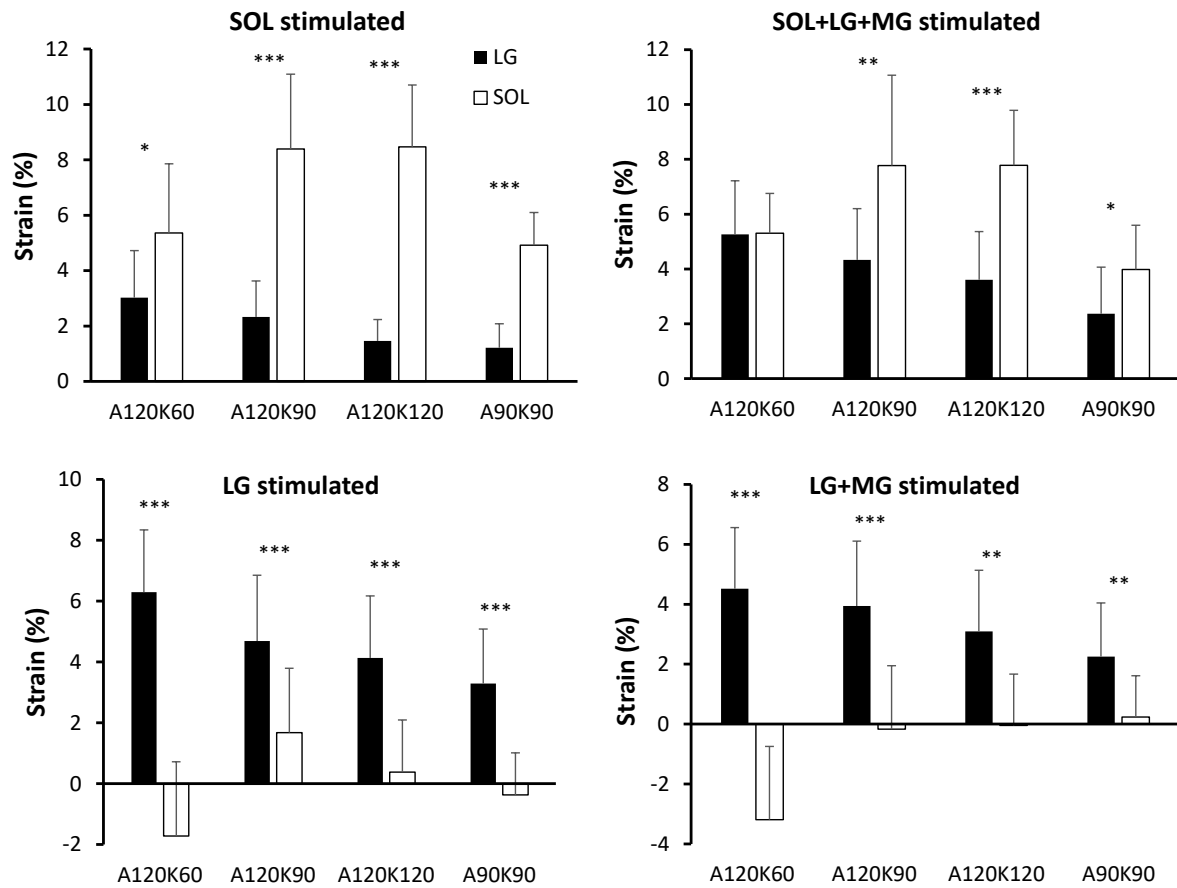


Figure 5. Effects of joint configuration and muscle stimulation condition on strain of soleus (SOL) and lateral gastrocnemius (LG) subtendons. Means + SD are shown (n = 12). Significant differences between SOL and LG subtendon strain: * p<0.05, ** p<0.01, *** p<0.001.

503

504